



## 29<sup>th</sup> International Conference on Lightning Protection

23<sup>rd</sup> – 26<sup>th</sup> June 2008 – Uppsala, Sweden



# LIGHTNING SIMULATION OF A COMBINED OVERHEAD LINE/CABLE CONNECTED GIS

Jakob Kessel, Víðir Atlason, Claus Leth Bak  
Institut of Energy Technology, Aalborg University  
[clb@iet.aau.dk](mailto:clb@iet.aau.dk)  
Pontoppidanstræde 101, DK-9220 Aalborg - Denmark

Jesper Lund  
NV Net A/S  
[jlu@nv.dk](mailto:jlu@nv.dk)  
Nefovej 50, 2. sal, DK-9310 Vodskov

**Abstract** – The following paper concerns different investigations of lightning simulation of a combined 170 kV overhead line/cable connected GIS. This is interesting due to the increasing amount of underground cables and GIS in the Danish transmission system. This creates a different system with respect to lightning performance, compared to a system consisting solely of AIS connected through overhead lines. The main purpose is to investigate whether overvoltage protection is necessary at the GIS busbar. Here, the price for a GIS SA is significantly more expensive than the price for an AIS SA. The analysis is conducted by implementing a simulation model in PSCAD/EMTDC.

Simulations are conducted for both SF and BFO where the overvoltages at the transformer are evaluated as this component has the lowest insulation strength. The overvoltages are evaluated for different front times of the lightning surge, different soil resistivities at the surge arrester grounding in the overhead line/cable transition and different length of the connection cable between the transformer and the GIS busbar with a SA implemented. Those simulations are conducted for different positions of the circuit breaker present at the GIS busbar. The lightning current required to cause inadmissible voltages at the transformer is evaluated and the MTBF is found for different cases. With the circuit breaker at the GIS busbar in closed position results indicate that SF does not cause inadmissible voltages to appear at the transformer. However, BFO caused by a lightning stroke of extremely high magnitude can cause inadmissible voltages to appear at the transformer. With the circuit breaker at the GIS busbar in open position results indicate that both SF and BFO can cause inadmissible voltages to appear at the transformer. A risk assessment based on the simulation results and statistical data for lightning, yields the conclusion that implementation of a surge arrester at the GIS busbar is not necessary.

## 1 INTRODUCTION

In accordance with the increased focus on visual pollution, the Danish transmission system is being exposed to great changes. Overhead lines (OHL) are being replaced with underground cables (UC) and air insulated substations (AIS) are being replaced with new less space consuming gas insulated substations (GIS). This is also the case for the 170 kV transmission system around Aalborg, where the objective is to replace most of the overhead lines with underground cables as well as rebuilding the substation in Aalborg East (ABØ) as an indoor GIS. This yields a different system with respect to lightning performance compared with a system consisting solely of AIS connected through OHL.

Though most of the system will consist of GIS and UC, and therefore not directly exposed to lightning, overvoltages due to lightning can still occur. Near the ABØ substation, an OHL section with two high towers across the Limfjord will still be present after the reconstruction of the system, resulting in a mixed OHL/UC section connecting to the ABØ GIS as shown in Fig. 1.

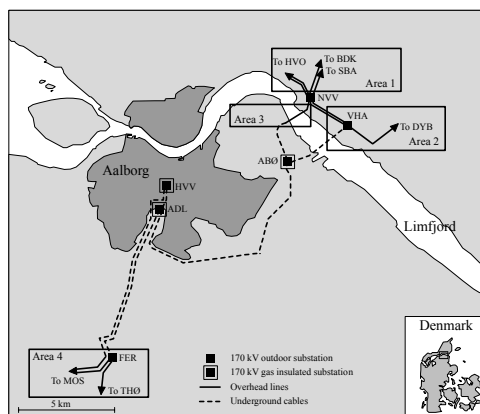


Fig. 1 – Geographical configuration of the 170 kV system in Aalborg, 2014.

In Fig. 1, the transmission system is divided into four areas where lightning can enter the system. In [1], it has been found that only lightning to area 3 can cause inadmissible voltages, hence this is the only area of interest in this paper.

Protection for a GIS is significantly more expensive than protection for an AIS (roughly with a factor of 10), it is therefore interesting to investigate whether overvoltage protection is necessary for the new GIS in ABØ.

This paper presents modelling and lightning simulation of the 170 kV transmission system in Aalborg. Both shielding failure (SF) and back flashover (BFO) are simulated, and the influence of different surge front times, different soil resistivities at the OHL/UC surge arrester (SA) transition point and the influence of different distances of the connection cable between the transformer and the busbar with a SA present are evaluated.

## 2 SYSTEM DESCRIPTION

A single line diagram of the transmission system around Aalborg is shown in Fig. 2, showing the relevant components of the system. As previously described, only lightning entering the OHL section O4 can cause inadmissible voltage. This is due to its close proximity to the ABØ substation and the fact that it contains two tall towers on each side of the Limfjord which are expected to attract a high number of lightning.

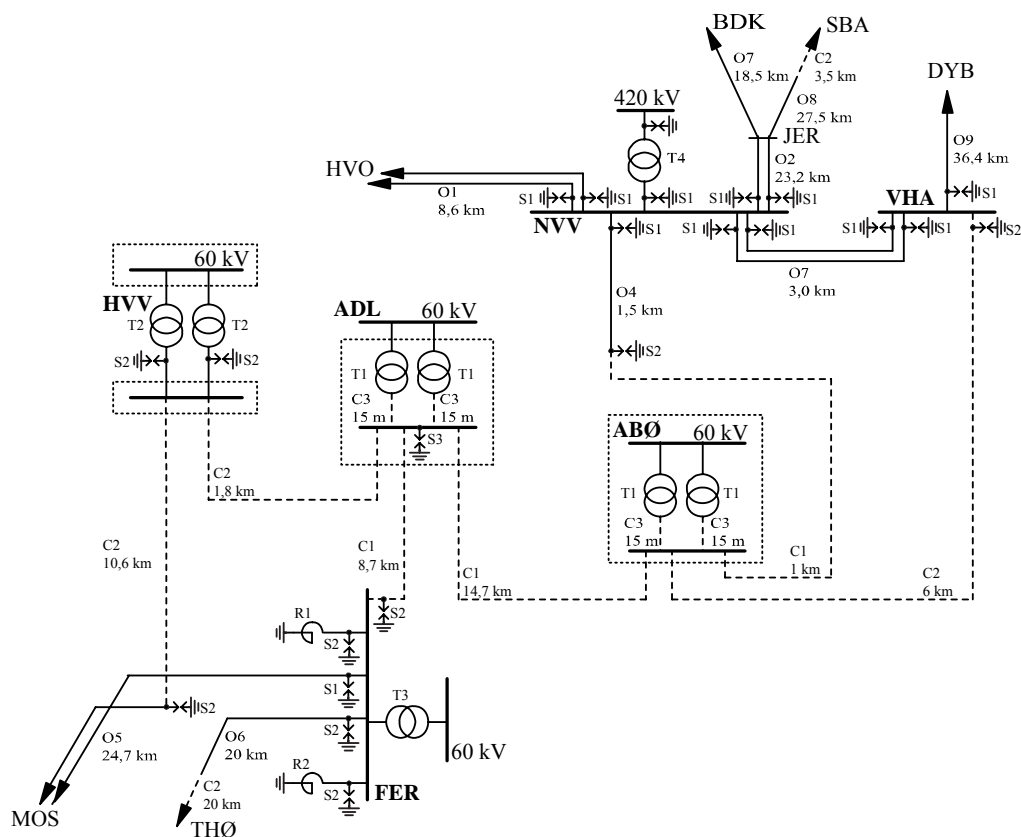


Fig. 2 – Single line diagram for the proposed system in 2014, containing the relevant parts. Substations and equipment enclosed with dotted lines are gas insulated.

Table 1 – Components in the single line diagram.

Figure label	Type
O1-O9	Overhead lines
C1-C3	Underground cables
S1-S3	Surge arresters
R1-R2	Reactors
T1-T4	Transformers

As OHL section O4 is the section of greatest interest, a more detailed description of the components in this section is given in the following.

**A. Lightning parameters**

The average lightning density in the Aalborg area is approximately 0,4 flashes to ground per km<sup>2</sup> per year. The lightning parameters are derived from measurements conducted on the mountain of San Salvatore in Switzerland [2].

**B. ABØ substation**

As previously described, the ABØ substation is to be reconstructed as a GIS with a single busbar and only UC entering the substation. A single line diagram of the proposed ABØ substation is shown in Fig. 3

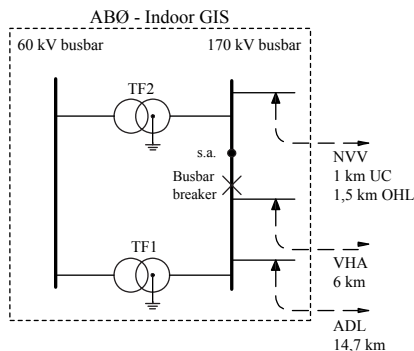


Fig. 3 – A single line diagram of the planned GIS in ABØ. *s.a.* represents a committed placement for the optional surge arrester.

**C. Underground cable ABØ-NVV**

Two different cable connection are entering the ABØ substation, namely C1 (NVV and ADL) and C2 (VHA). Both cable types are single phase cables. C1 (AXLJ 1x2000mm<sup>2</sup>) represents a flat physical layout, with 2000 mm<sup>2</sup> Al conductors, with a surge impedance of 20,5 Ω. C2 (AXLJ 1x1200mm<sup>2</sup>) represents a triangular physical layout, with 1200 mm<sup>2</sup> Al conductors, with a surge impedance of 23,4 Ω.

**D. Overhead line section O4**

The OHL leading from NVV to the UC is 1,5 km long as shown in Fig. 2. This section contains two towers with a total height of 145 m as shown in Fig. 4. As shown a 420 kV system is present at the same tower above the 170 kV system.

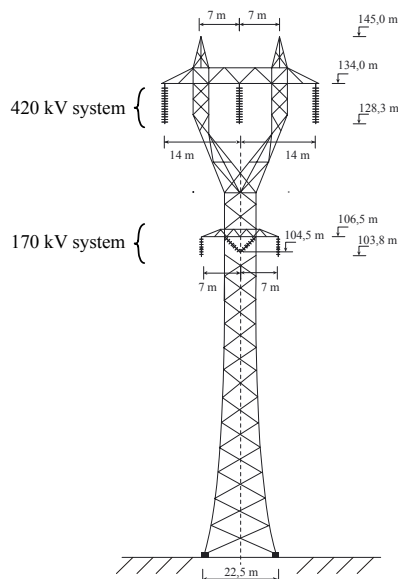


Fig. 4 – Illustration of the tower profile used in section O4.

The Lightning Impulse Withstand Level (LIWL) of the 170 kV insulators is 750 kV and the LIWL for the 420 kV insulators is 1425 kV.

### E. Surge Arresters at the OHL/UC transition point

At the OHL/UC transition point, a SA is implemented for each phase. These SA are of the type ABB Pexlim P144XV170, line discharge class 4 (IEC), with nominal discharge current of 20 kA. Discharge current withstand strength: High current 4/10  $\mu$ s, 100 kA<sub>peak</sub>; Low current 2000  $\mu$ s 1350 A<sub>peak</sub>. The discharge characteristics of the SA are given in Fig. 6.

### F. Grounding electrode system

The grounding electrodes in the system are single Cu rods, length 6 m, radius 5,5 mm.

## 3 MODELLING

The simulation model of the above-mentioned system is implemented in PSCAD/EMTDC as presented in the following. Generally following the guidelines stated in [3].

### A. Transmission lines

All OHL and UC in the system are modelled by use of the *Frequency dependent (phase) model* and implemented by use of the physical configuration as suggested in [4].

### B. Substations

AIS busbars are modelled by transmission lines with the physical configuration. GIS busbars are modelled by their equivalent capacitances. This is done to avoid heavy simulation, due to short length of the GIS busbars.

### C. Transformers and reactors

The transformers and reactors at the substations are modelled by their equivalent capacitances according to [3].

### D. Voltage source

The voltages at each phase for both the 170 kV and 420 kV are implemented with a DC supply with the corresponding instantaneous AC voltages.

### E. Surge generator

The lightning surge generator is implemented with three inputs: the front time, the time to half and crest magnitude of the lightning current. The lightning surge is based on an approximated double exponential function [5]:

$$f(t) = \exp(-B \cdot t) - \exp(-A \cdot t) \quad (1)$$

Here, the constants  $B$  and  $A$  determine the front and tail time of the double exponential surge. The magnitude of the lightning surge is multiplied with  $f(t)$ .

### F. Surge arrester

A frequency dependent model for the SAs in the system is desired. For this purpose, a simplified version of the IEEE model, presented by Pinceti et al. [6], is used as shown in Fig. 5.

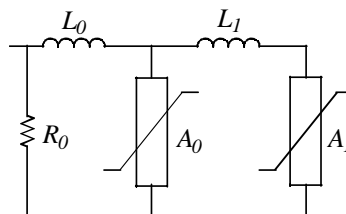


Fig. 5 – Simplified IEEE prepared by Pinceti et al. [6].

The inductances  $L_0$  and  $L_1$  characterize the frequency dependency of the SA, with respect to lightning current surges. The parameters are determined by a simplified method [7]:

$$\begin{aligned} L_0 &= 0,01 \cdot U_n \\ L_1 &= 0,03 \cdot U_n \end{aligned} \quad (2)$$

Where  $U_n$  is the rated voltage of the SA.

The input resistance is implemented for numerical stability and is given a general value of  $1 \text{ M}\Omega$  [6]. The conductances, which represent the non-linear characteristics of the SA, are found from general values given by [6]. These values are adjusted in order to obtain a discharge characteristic which fit data from SA producer. The conductances are implemented in EMTDC/PSCAD with the values listed in Table 2.

Table 2 – The parameter values for the conductances in the SA model.

Current [kA]	$A_0$ [p.u. of $U_n$ ]	$A_1$ [p.u. of $U_n$ ]	Current [kA]	$A_0$ [p.u. of $U_n$ ]	$A_1$ [p.u. of $U_n$ ]
0,001	0,0001	0,0001	8,000	1,170	0,987
0,010	0,805	0,755	10,00	1,190	1,005
0,100	0,960	0,820	14,00	1,240	1,053
1,000	1,060	0,867	18,00	1,265	1,088
2,000	1,098	0,898	20,00	1,274	1,100
4,000	1,138	0,939			

The discharge characteristics of the implemented model are compared with the discharge characteristics given by the SA producer [8]. This comparison is shown in Fig. 6 evaluated for an  $8/20 \mu\text{s}$  surge current.

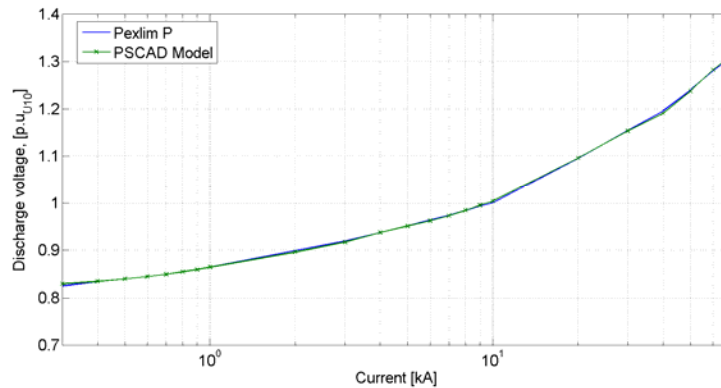


Fig. 6 – Comparison of discharge characteristic for a  $8/20 \mu\text{s}$  surge current for the model and producer data.

As shown, the SA model corresponds to the provided data for the  $8/20 \mu\text{s}$  waveform.

### G. Grounding resistance

The grounding resistance is modelled as described in [9] and [10]. The grounding resistance is dependent on the magnitude of the current flowing to ground and the actual resistance for low magnitude currents. The current dependent resistance is determined by:

$$R_t = \frac{R_0}{\sqrt{1 + \frac{I_R}{I_g}}} \quad \text{where: } I_g = \frac{E_0 \rho}{2\pi R_0} \quad (3)$$

Where:

$R_0$  is the low current grounding resistance

$I_R$  is the peak value of the current flowing through the ground resistance.

$I_g$  is the critical current causing ionization of the soil

The low current grounding resistance is found from the soil resistivity and physical dimensions of the grounding rod [11]:

$$R_0 = \frac{\rho}{2\pi l} \left[ \ln \frac{4 \cdot l}{r} - 1 \right], \quad \text{for } l \gg r \quad (4)$$

Where:

- $\rho$  is the soil resistivity
- $l$  is the length of the grounding rod
- $r$  is the radius of the grounding rod

The grounding resistance is implemented for the grounding of the SA at the OHL/UC transition and for the grounding of the towers which are described in the following.

**H. Tower model**

The tower model is based on the principle described in [3] and shown in Fig. 7. Here, one ground wire is placed above the three phase conductors. The insulators between the crossarm of the tower and the phase conductors are modelled with equivalent capacitances. If a flashover across the insulator occurs, the capacitance is short circuited. The tower is represented with an equivalent surge impedance [12]-[13] and the grounding resistance is dependent on the current flowing to ground as previously presented.

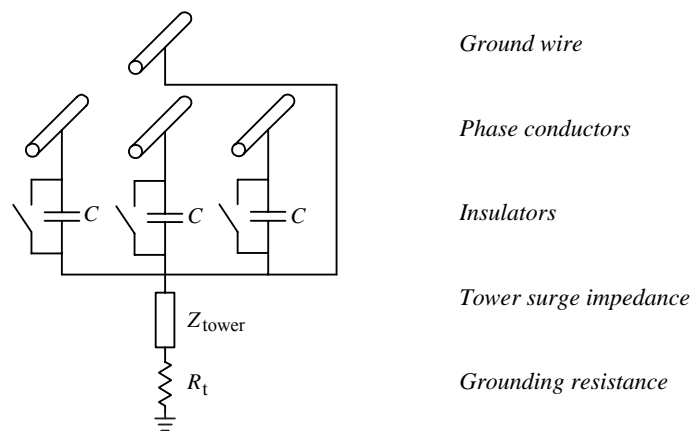


Fig. 7 – A principle drawing of the tower model [14] showing a ground wire above the phase conductors, insulators, tower and grounding resistance.

In the simulation model, a tower component is created following the principle presented above. The tower in OHL section O4 has a height of 145 m and the surge impedance is divided into three parts as shown in Fig. 8. This is done to implement the effect of different heights of the 420 kV and 170 kV system on the tower, respectively.

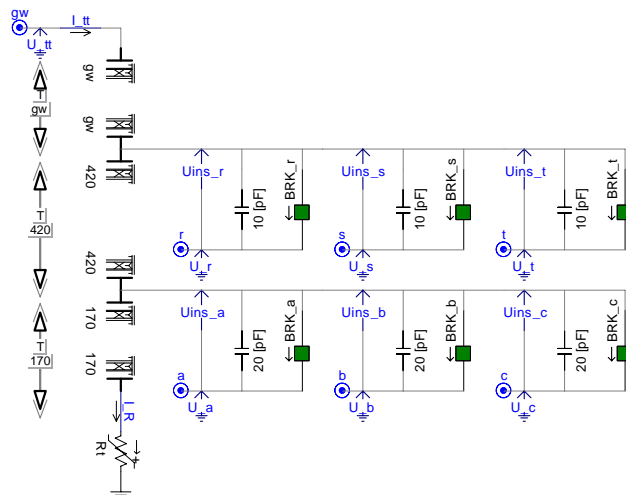


Fig. 8 – The implemented tower model in PSCAD/EMTDC, showing the tower component and insulator. Breaker control for insulator flashover is not shown here.

The insulator model is implemented for both the 170 kV and the 420 kV system. For the 170 kV system, a capacitance of 20 pF is chosen to represent the insulator, and for the 420 kV system a 10 pF capacitance is used, in

accordance with [3]. Here the breakdown is implemented from an estimated volt-time characteristic of the insulator [14]:

$$U_{\text{breakdown}} = K_1 + \frac{K_2}{t^{0.75}} \quad (5)$$

Where:

$U_{\text{breakdown}}$  is the breakdown voltage of the insulator

$K_1 = 400 \cdot l$

$K_2 = 710 \cdot l$

$l$  is the length of the insulator

$t$  is the time elapsed after the lightning surge

### I. Simulation model implemented in PSCAD/ EMTDC

The model is implemented in PSCAD/EMTDC as shown in Fig. 9.

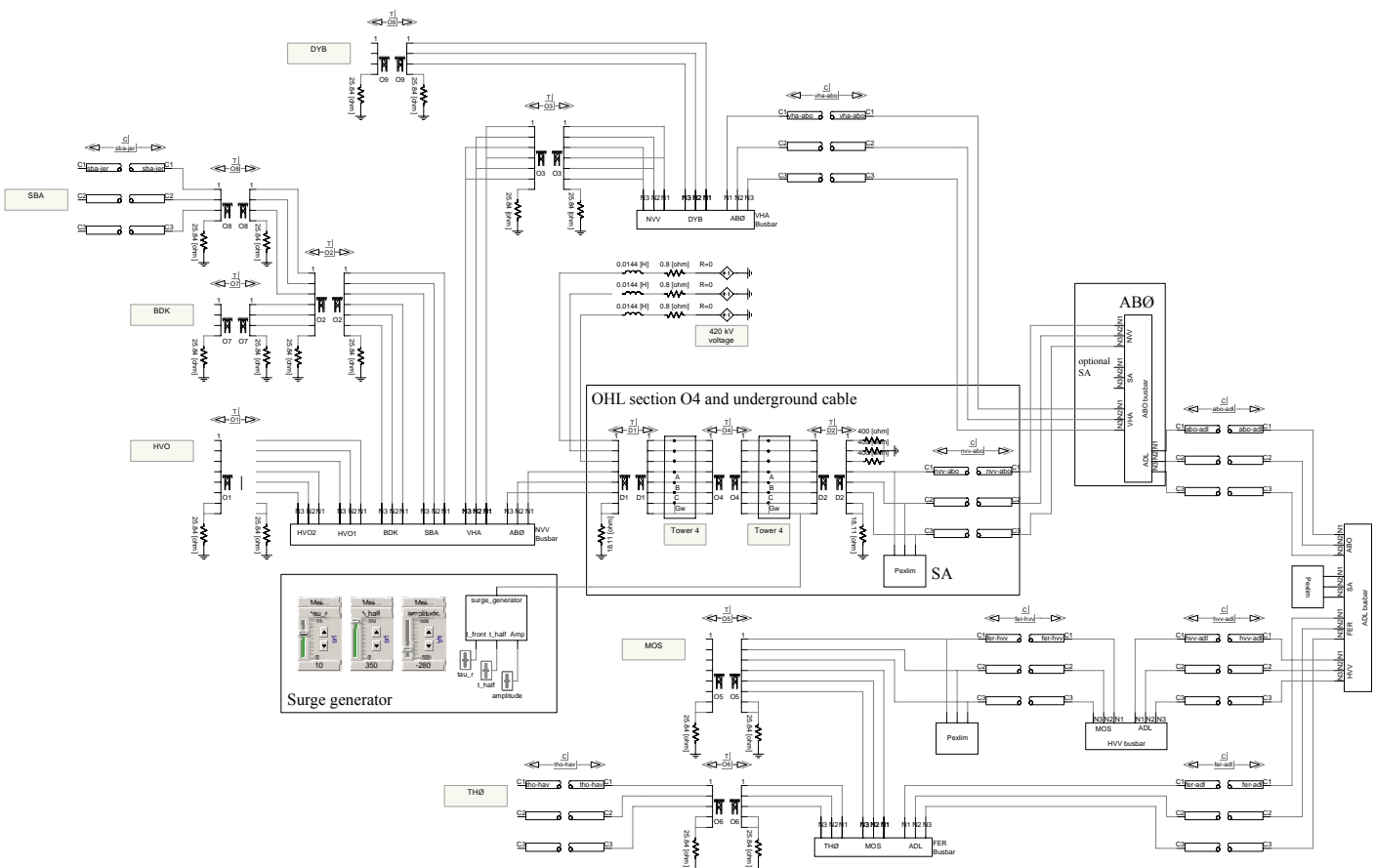


Fig. 9 – The full simulation model of the 170 kV transmission system in Aalborg. All substations are implemented as enclosed subsystems, surge arresters in the system are likewise implemented as subsystems, in most cases implemented inside a substation. At the ABØ substation an optional surge arrester can be implemented. The OHL section O4 is implemented with 3 transmission lines with the two towers implemented in between. The lightning surge generator is implemented as a subsystem, where front time, time to half and crest magnitude can be adjusted. Further description of the modelling of the system is given in [1].

## 4 SIMULATION

The transformers placed in ABØ have a LIWL of 650 kV, hence, the maximum allowable voltage appearing at the terminals is determined from safety factor of 15% (IEC) to be 565 kV. As the busbar breaker position is included in the analysis, four different cases are simulated:

- Shielding failure with the breaker at the busbar in ABØ in closed position.
- Shielding failure with the breaker at the busbar in ABØ in open position.

- Back flashover with the breaker at the busbar in ABØ in closed position.
- Back flashover with the breaker at the busbar in ABØ in open position.

Fig. 10 gives an overview of the OHL/UC configuration. The lightning is simulated to strike to the tower (BFO) or near the tower (SF) closest to the GIS. Surge arresters are implemented at all phases, at the OHL/UC transition point, before the 1 km long UC connecting to the GIS.

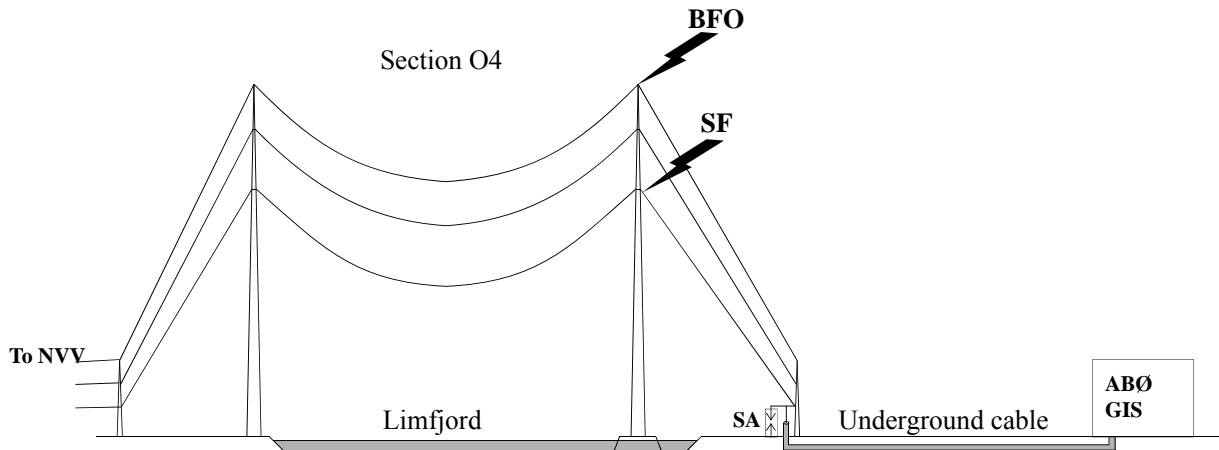


Figure 10 – Principle overview of the system settings.

The SF is simulated by applying a negative lightning surge to a phase conductor. The amplitude of the lightning surge which can occur at SF has been determined to have a maximum value of -41,8 kA by use of "geometric model of the last step of the lightning stroke" [11]. As a SF will occur at a random voltage of the power frequency [16], it is chosen to use the peak voltage of the power frequency with the same polarity as the lightning surge, in order to represent a worst case. Unless otherwise stated, SF is simulated with the parameters defined in Table 3. The front times of the lightning surge during SF are found from the correlation between lightning current magnitude and rate of rise, given by [15]:

$$t_{\text{front}} = \frac{I}{24 \cdot \left(\frac{1}{P} - 1\right)^{0.25}} \quad (6)$$

In equation 6,  $I$  is the lightning current crest magnitude and  $P$  is the probability of a crest current exceeding the magnitude of  $I$ . As the front time is the most important factor for the overvoltages appearing at the transformer terminals, it is chosen to use the same time to half for the simulation of SF and BFO.

The BFO is simulated by applying a negative lightning surge to the tower top, and unless otherwise stated with simulation parameters as shown in Table 3. The lightning parameters for simulation of BFO are recommended by IEC.

Table 3 – Simulation parameters.

	Front time [μs]	Time to half [μs]	Crest magnitude [kA]	Soil resistivity [Ωm]
SF	1,4	350	-41,8	92,5
BFO	10	350	-200	92,5

With the parameters presented in Table 3, simulation of both SF and BFO with open and closed breaker is conducted. With the breaker in closed position, the same voltages are recorded at both transformer terminals. With the breaker in open position, the voltages appearing at transformer 2 (TF2 in Fig. 3) are more critical, as the incoming surge is entering the busbar at the same side of the breaker as TF2. The recorded voltages at TF2 are shown in Fig. 11 and Fig. 12.



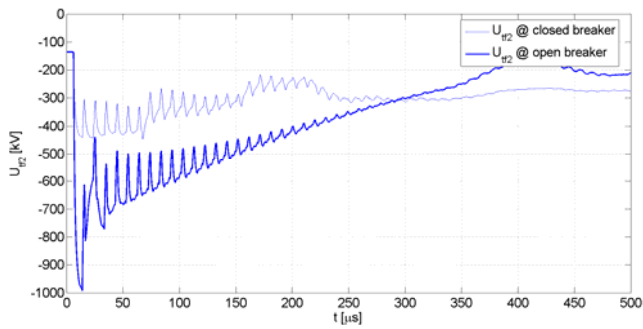


Fig. 11 – Simulation of a -41,8 kA 1,4/350  $\mu$ s SF.

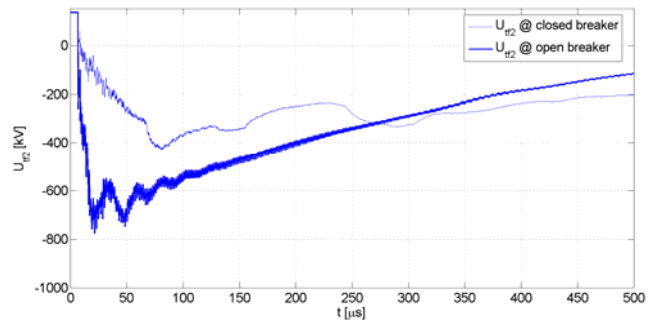


Fig. 12 – Simulation of a -200 kA 10/350  $\mu$ s BFO.

From the simulation results, it can be seen that inadmissible voltages, defined to be 565 kV, do appear at the TF2 terminals when the breaker at the busbar is in open position. With the breaker in closed position, neither SF nor BFO caused inadmissible voltages to appear at the TF2 terminals. In order to analyse the influence of different parameters the following investigations are conducted:

- The front time of the lightning surge during SF.
- The soil resistivity at the OHL/UC transition point.
- Length of the connection cable between busbar and TF2, with a SA implemented at the busbar.

All simulation results shown in the following, concern SF as these give clearer viewing of the propagated waveshapes appearing at the TF2, due to lesser reflections. An evaluation of lightning currents causing failure is conducted later in the paper concerning both SF and BFO.

**A. Effect of surge front time at SF**

The following simulation concerns SF and the influence of different front times on the voltages appearing at TF2. The simulation is conducted with the parameters shown in Table 3, only with varying front times as listed in Table 4.

Table 4 – The lightning current front times.

Front time [ $\mu$ s]	1	2,5	5	7,5	10
-----------------------	---	-----	---	-----	----

The simulation results for SF, with varying front time are shown in Fig. 13 and Fig. 14.

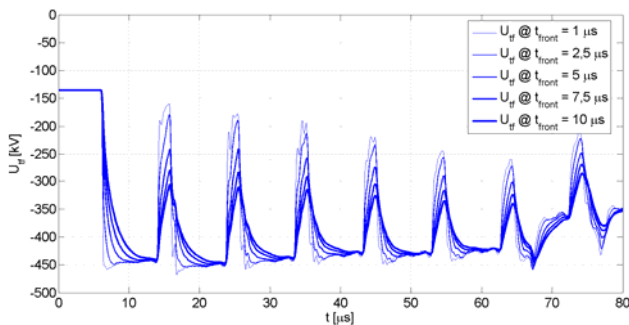


Fig. 13 – Varying lightning front time, SF, closed breaker.

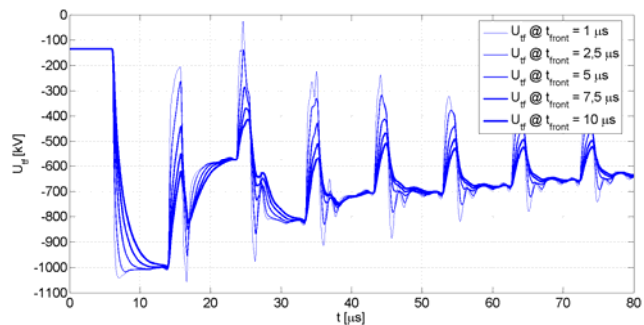


Fig. 14 – Varying lightning front time, SF, open breaker.

The simulation results, with different front times yielded only slight differences in voltage amplitude, measured at the TF2, as shown in Fig. 13 and Fig. 14. This indicates that the steepness of the lightning surge is not a factor of great importance for lightning entering the system at this point, for  $t_{front} < 10 \mu$ s. This is due to the length of the cable leading into the substation which has a length of 1 km, where the propagation time is estimated to be approximately 5  $\mu$ s. Hence, all surges have reached their crest value before a reflected wave returns and dampens the incoming surge. With the breaker at the busbar in closed position, voltages at the TF2 terminals did not reach inadmissible levels, defined to be 565 kV. With the breaker at the busbar in open position inadmissible voltage stress was recorded for all examined front times.

### B. Effect of soil resistivity at the OHL/UC transition point during SF

The influence of different soil resistivities, at the OHL/UC SA grounding point, on the voltages appearing at the TF2 are investigated during SF. The simulation is conducted with the parameters shown in Table 3, only with varying soil resistivity as listed in Table 5.

Table 5 – The soil resistivities with corresponding low current resistance  $R_0$  and critical current  $I_g$ .

$\rho$ [ $\Omega\text{m}$ ]	10	50	100	200	500	1000
$R_0$ [ $\Omega$ ]	1,96	9,8	19,6	39,2	97,9	195,8
$I_g$ [kA]	166	33,2	16,6	8,3	3,3	1,7

The simulation results for SF, with varying soil resistivity are shown in Fig. 15 and Fig. 16.

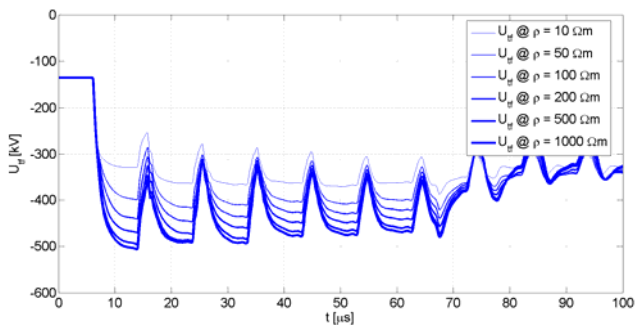


Fig. 15 – Varying soil resistivity, SF, closed breaker.

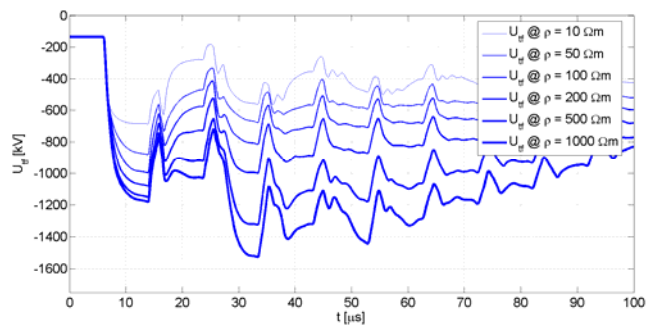


Fig. 16 – Varying soil resistivity, SF, open breaker.

As shown in Fig. 15 and Fig. 16, the simulation results with different soil resistivities yielded great differences in voltage amplitude at TF2 for both closed and open breaker, indicating the importance of this factor for the model validity. With the breaker at the busbar in closed position, voltages at TF2 did not reach inadmissible levels. With the breaker at the busbar in open position inadmissible voltage stress was recorded for all simulation cases.

### C. Effect of the cable length between GIS busbar and TF2 during SF, with a SA implemented at the GIS busbar

The effect of the length of the connection cable between the GIS busbar and TF2 is evaluated with a SA implemented at the GIS busbar. The simulation is conducted with the lightning parameters shown in Table 3 and a SA, with the same discharge characteristics as the SA described on page 4, implemented at the GIS busbar in the simulation model. Only the length of the connection cable is varied as listed in Table 6.

Table 6 – Length of cable between transformer and busbar.

Cable length [m]	5	15	30	50	100	150	200
------------------	---	----	----	----	-----	-----	-----

The most important factors determining the voltage appearing at TF2, are the steepness of the lightning surge and the cable length between the SA and the equipment which is to be protected. Here, the steepness is kept constant with a rise time of 1,4  $\mu\text{s}$ , while varying the cable length from 5 to 200 m. The results are shown in Fig. 17 and Fig. 18.

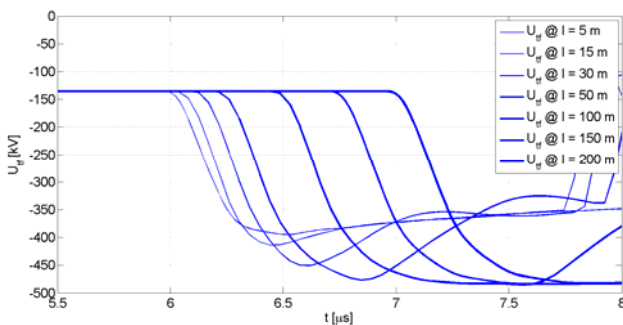


Fig. 17 – Varying cable length to transformer, SF, closed breaker.

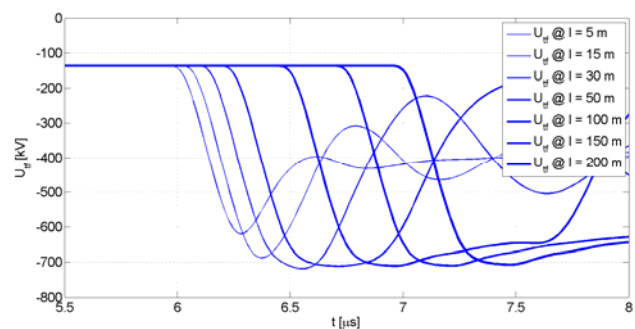


Fig. 18 – Varying cable length to transformer, SF, open breaker.

The simulation results with different cable lengths yielded differences in the voltages at TF2, as shown in Fig. 17 and Fig. 18, indicating the importance of this factor for the protection of the transformer. With the breaker at the busbar in closed position, voltages at TF2 did not reach inadmissible levels. With the breaker at the busbar in open position inadmissible voltage stress was recorded for all cases of cable length. Furthermore, cable length exceeding 50 m did not yield increased voltage stress of TF2. This is due to the steepness of the residual surge wave and travelling time across the cable, where the residual surge has reached its crest value before it has travelled 50 m. Here, the residual surge wave is the surge passing the SA towards TF2.

**5 EVALUATION OF CURRENTS CAUSING INADMISSIBLE VOLTAGES AT TF2**

In order to decide whether further protection of the GIS equipment is necessary, an evaluation of lightning currents causing inadmissible voltages is needed. The case of inadmissible voltages at TF2 is defined as failure. This is evaluated for the different cases in the following.

**A. Currents causing in admissible voltages for varying front time**

The currents required to cause failure are evaluated for SF with different front times. The correlation between the front time and the current amplitude is shown in Fig. 19. Here, only a SF with the breaker in open position caused a failure.

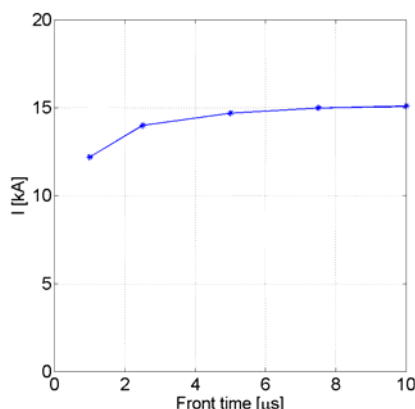


Fig. 19 – Current vs. front time, SF, open breaker.

Fig. 19 shows the effect of lightning surge front times on the currents required to cause failure, where it is apparent that slower surge fronts require higher current crest magnitude to cause failure.

**B. Currents causing inadmissible voltages for varying soil resistivity**

The lightning currents required to cause failure are estimated for SF and BFO with different soil resistivities at the OHL/UC transition point. No failures were recorded for SF, with the breaker at the busbar in closed position. However, failures were recorded for SF, breaker in open position, and BFO with breaker in open and closed position. The results are shown in Fig. 20, Fig. 21 and Fig. 22.

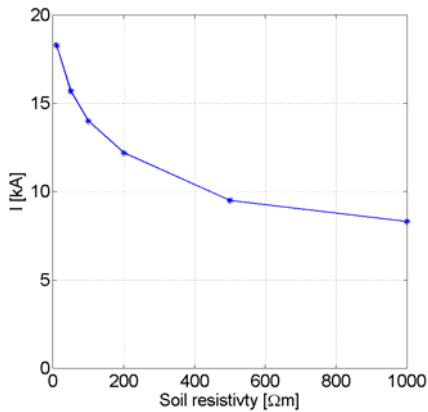


Fig. 20 – Current vs. soil resistivity, SF, open breaker.

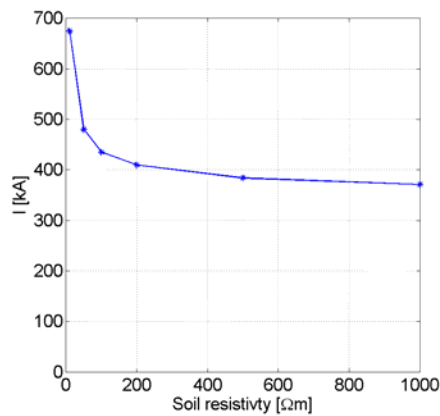


Fig. 21 – Current vs. soil resistivity, BFO, closed breaker.

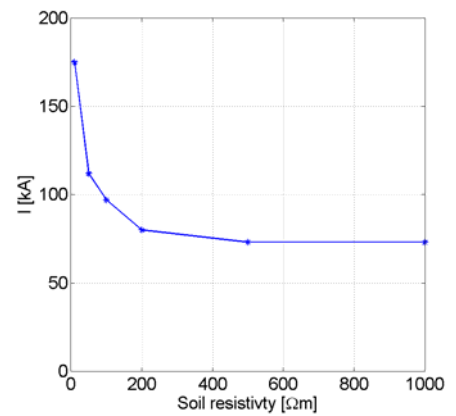


Fig. 22 – Current vs. soil resistivity, BFO, open breaker.

The currents required to cause failure are shown as a function of the soil resistivity in the three figures above. As shown, the quality of the grounding affects the magnitude of the currents causing failure. Better grounding (lower soil resistivity) requires a higher current magnitude to cause failure. Furthermore, it can be seen that  $\rho > 500 \Omega\text{m}$  does not yield significant changes in currents required to cause failure.

### C. Currents causing inadmissible voltages for varying cable length between GIS busbar and TF2

The lightning currents required to cause a failure are evaluated for varying length of the connection cable between the busbar, where a SA is implemented at the busbar. For this case, failure was only recorded with the busbar breaker in open position, both for SF and BFO. The resulting currents for varying cable lengths are shown in Fig. 23 and Fig. 24.

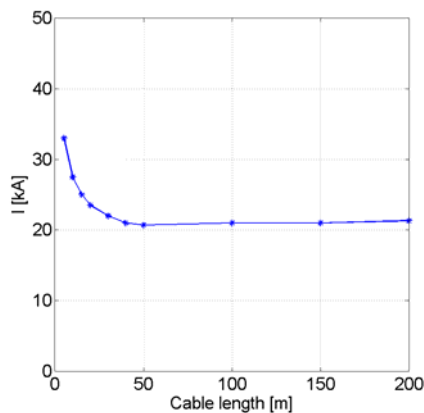


Fig. 23 – Current vs. cable length, SF, open breaker.

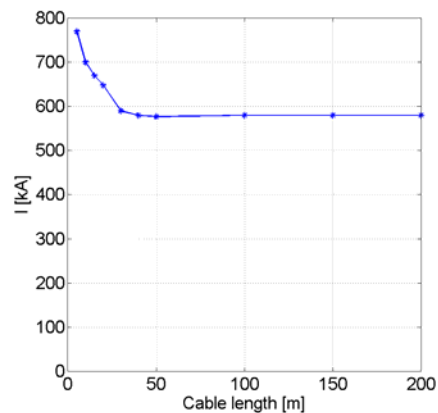


Fig. 24 – Current vs. cable length, BFO, open breaker.

The currents required to cause failure are shown as a function of the length of the connection cable between the busbar and the transformer. As shown, higher currents are required to cause failure for shorter cables. For cables above 50 m, approximately the same current is required to cause failure.

## 6 RISK ASSESSMENT

The risk assessment is conducted by defining mean time between failure (MTBF), where failure is defined as the appearance of a voltage surge, exceeding the allowable limit of 565 kV at the transformer terminals. In order to evaluate the MTBF, the number of lightning in the area is needed as well as the crest current probability and the probability of a given breaker position. Furthermore, when evaluating MTBF for SF, the probability of a shielding failure in the given system is required. Acceptable MTBF for a GIS is defined in [17] to be in the region of 250-1000 years, where in this case the higher value set as a limit.

The MTBF for the four cases are calculated with the following equations:

$$MTBF_{SF, closed} = (P(sf) \cdot P(closed) \cdot P(current) \cdot N_{flashes})^{-1} \quad (7)$$

$$MTBF_{SF, open} = (P(sf) \cdot P(open) \cdot P(current) \cdot N_{flashes})^{-1} \quad (8)$$

$$MTBF_{BFO, closed} = (P(closed) \cdot P(current) \cdot N_{flashes})^{-1} \quad (9)$$

$$MTBF_{BFO, open} = (P(open) \cdot P(current) \cdot N_{flashes})^{-1} \quad (10)$$

The number of flashes to the section is  $N_{flashes} = 0,32$  flashes/yr.

The probability of a shielding failure is estimated,  $P(sf) = 0,02$ .

The probability of the breaker being in open position is estimated,  $P(open) = 1/365 = 0,0027$ .

The probability of the breaker being in closed position is  $P(closed) = 1 - P(open) = 0,9973$ .

The probability of a lightning with a current magnitude of  $I$  or greater is given by [15]:

$$P(current) = \frac{1}{1 + \left(\frac{I}{31}\right)^{2,6}} \quad (11)$$

The probability of the current is given as the difference between the probability of the minimum current which can cause failure and the maximum current which can cause a SF.

$$P(current) = P(min) - P(max) \quad (12)$$

The MTBF calculated for all the simulation cases yielding failure and the results are shown in the following.

#### A. MTBF for varying lightning surge front time

As previously described, the relationship between the current required to cause failure and the front time of the lightning surge was found. From this evaluation, the MTBF is calculated for the varying lightning surge front time with the corresponding results shown in Fig. 25.

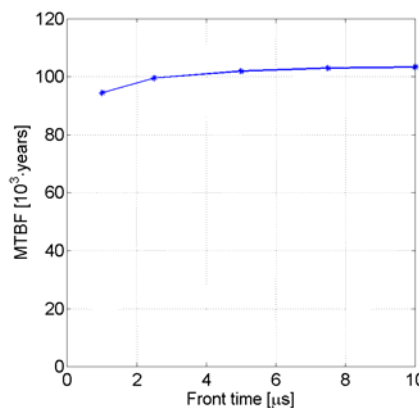


Fig. 25 – MTBF vs. front time, SF, open breaker.

The  $MTBF_{SF, open}$  for varying front times show an estimated  $MTBF > 90.000$  years.

#### B. MTBF for varying soil resistivity of the OHL/UC transition point

Based on the evaluation of required currents to cause failure, the MTBF can be found for varying soil resistivity at the OHL/UC transition point (SA grounding). The results are shown in Fig. 26, Fig. 27 and Fig. 28.

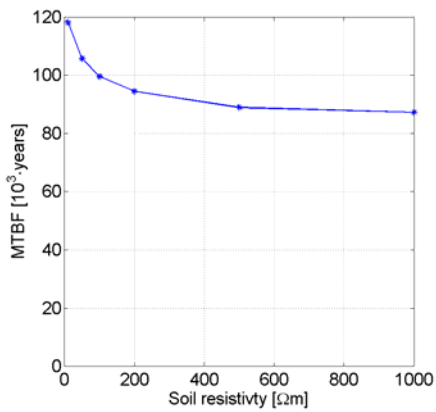


Fig. 26 – MTBF vs. soil resistivity, SF, open breaker.

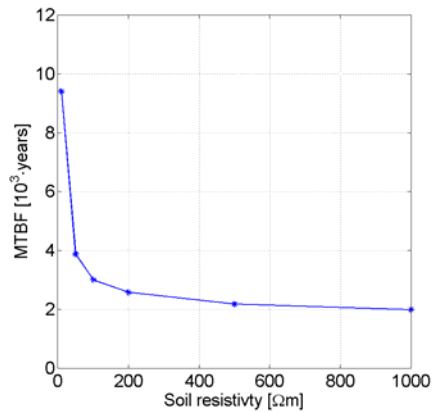


Fig. 27 – MTBF vs. soil resistivity, BFO, closed breaker.

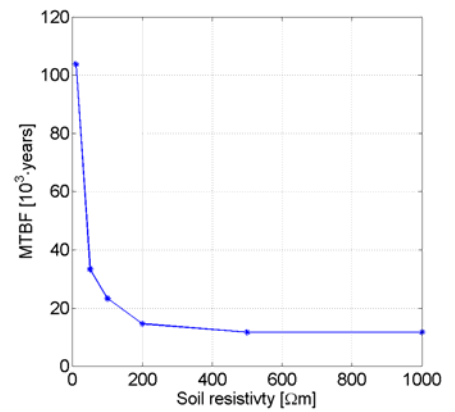


Fig. 28 – MTBF vs. soil resistivity, BFO, open breaker.

The  $MTBF_{SF,open}$  for varying soil resistivity, show an estimated  $MTBF > 80.000$  years

The  $MTBF_{BFO,closed}$  for varying soil resistivity, show an estimated  $MTBF > 2.000$  years.

The  $MTBF_{BFO,open}$  for varying soil resistivity, show an estimated  $MTBF > 10.000$  years.

### C. MTBF for varying distance between transformer and busbar

Based on the evaluation of required currents to cause failure, the MTBF can be found for varying distances of the connection cable between the busbar and the transformer, with a SA implemented at the busbar. The results are shown in Fig. 29 and Fig. 30.

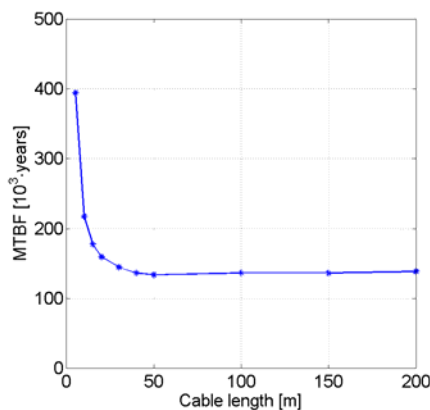


Fig. 29 – MTBF vs. distance, SF, open breaker.

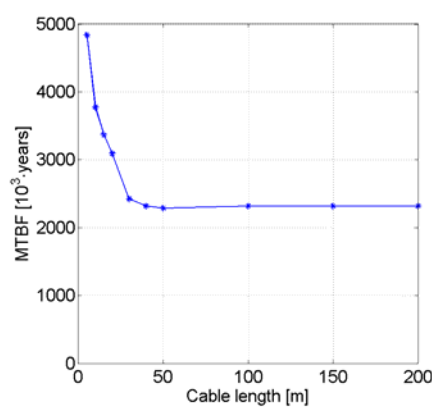


Fig. 30 – MTBF vs. distance, BFO, open breaker.

The  $MTBF_{SF,open}$  for varying cable length, show an estimated  $MTBF > 100.000$  years.

The  $MTBF_{BFO,open}$  for varying cable length, show an estimated  $MTBF > 2.000.000$  years.

As shown in the previous section, all estimated MTBF are above the acceptable limit of 1.000 years.

## 7 CONCLUSION

This paper concerns a lightning simulation of a system containing a GIS, where all connections are in the form of UC. The voltage experienced at TF2 was investigated for both SF and BFO with open and closed breaker at the busbar. Furthermore, the influence of three different parameters was investigated. From the simulation, cases yielding inadmissible voltages appearing at TF2 were defined as critical.

- *The steepness of the lightning surge did not prove to be a parameter of significance for this system. This is due to the length of the cable leading into the substation, as all simulated lightning surges have reached their crest value before a reflected wave reaches the OHL/UC transition point.*
- *The soil resistivity of the OHL/UC transition point, where a SA is implemented, did prove to be a factor of significance. As expected, improved grounding at this point resulted in a decrease of the voltage appearing at TF2, due to a lower SA residual voltage.*
- *The influence of the cable length between transformer and the SA implemented at the GIS busbar was investigated by simulation of critical cases. Increased cable length yielded increased voltage magnitude to appear at the transformer terminals, for cable lengths up to 50 m. This is due to the fact that the residual surge has reached its crest value before it has travelled 50 m.*

A risk assessment was conducted for the cases defined as critical, yielding a MTBF above the acceptable limit of 1.000 years for all cases.

The conclusion from this investigation of lightning to a mixed OHL-UC transmission system is that the UC connecting to the substation along with the SA in the OHL/UC transition point provides adequate protection for the GIS equipment. Further protection in the form of SA at the GIS busbar is therefore not necessary.

## 8 REFERENCES

- [1] Jakob Kessel, Viðir Atlason, Mariusz Benesz, "Analysis and simulation of lightning performance of the 150 kV system in Aalborg". IET, AAU 2008. This project is available at the institute secretary Maria Hald ([mha@iet.aau.dk](mailto:mha@iet.aau.dk)) at IET, AAU.
- [2] K. Berger, R.B. Anderson, "Parameters of Lightning Flashes". Cigré Electra, No. 41, p. 23-37, 1975.
- [3] Fast Front Task Force of the IEEE Modeling and Analysis of System Transients Working Group, "Modeling guidelines for fast front transients", IEEE, 1997.
- [4] J.A. Martinez, F. Castro-Aranda, "Lightning Flashover Rate of an Overhead Transmission Line Protected by Surge Arresters", IEEE 2007.
- [5] F. Heidler, J. M. Cvetic, B. V. Stanic, "Calculation of Lightning Current Parameters", IEEE Transactions on Power Delivery, Vol. 14, No. 2, April 1999.
- [6] P. Pinceti, M. Giannettoni, "A simplified model for zinc oxide surge arresters", IEEE Transactions on Power Delivery, Vol. 14, No. 2, April 1999.
- [7] M. C. Magro, M. Giannettoni, P. Pinceti, "Validation of ZnO Surge Arresters Model for Overvoltage Studies", IEEE Transactions on Power Delivery, Vol. 19, No. 4, October 2004.
- [8] ABB Power Technologies, "High Voltage Surge Arresters, Buyer's Guide". ABB, 2007. Edition 5.1, 2007-04.
- [9] M. M. Osborne, A. Xemard, L. Prikler, J. A. Martinez, "Points to consider regarding the insulation coordination of GIS substations with cable connections to overhead lines", IPST 2007.
- [10] W. A. Chisholm, W. Janischewskyj, "Lightning Surge Response of Ground Electrodes", IEEE Transactions on Power Delivery, Vol. 4, No. 2, April 1989.
- [11] A. R. Hileman. "Insulation Coordination for Power Systems". CRC Press, 1999. ISBN: 0-8247-9957-7.
- [12] Working Group on Lightning Performance of Transmission Lines, "A Simplified Method for Estimating Lightning Performance of Transmission Lines", IEEE Transactions on Power Apparatus and Systems, Vol. PAS-104, No. 4, April 1985.
- [13] M. A. Sargent, M. Darveniza, "Tower Surge Impedance", IEEE Transactions on Power Apparatus and Systems, Vol. Pas-88, No. 5, May 1969.
- [14] P. Yadee and S. Premrudeepreechacharn, "Analysis of Tower Footing Resistance Effected Back Flashover Across Insulator in a Transmission System", IPST 2007.
- [15] H. M. Ryan. "High voltage engineering and testing". Peter Peregrinus Ltd. 1<sup>st</sup> edition, 1994. ISBN: 0-86341-293-9.
- [16] IEC, "Insulation Coordination. Part 2: Application guide". CEI, 1996, 3<sup>rd</sup> edition.
- [17] IEC, "Surge Arresters. Part 5: Selection and application recommendation". CEI, 1996, 1<sup>st</sup> edition.